Inorganic Chemistry

Article

pubs.acs.org/IC

Environmental Sensitivity of Ru(II) Complexes: The Role of the Accessory Ligands

Eileen N. Dixon,[†] Michael Z. Snow,[†] Jennifer L. Bon,[†] Alison M. Whitehurst,[†] Benjamin A. DeGraff,*[,†] Carl Trindle,[‡] and James N. Demas[‡]

[†]Department of Chemistry, James Madison University, Harrisonburg, Virginia 22807, United States

[‡]Department of Chemistry, University of Virginia, Charlottesville, Virginia 22901, United States

Supporting Information

ABSTRACT: A suite of Ru(II) complexes in which one ligand is pH responsive and the other two are varied in an effort to achieve improved photophysics has been synthesized and their potential as pH reporters assessed. The more general purpose of the study was to examine the role of the accessory ligands in heteroleptic reporter complexes and the degree to which such ligands can affect the performance of luminescent reporters. For this suite of complexes, judicious choice of the accessory ligand can alter both the pK_a* and the dynamic range of response. It was found that the emission color and brightness were influenced by pH, but the lifetimes were only weakly affected. Surprisingly, some accessory ligands which should have improved luminescent properties essentially turned off the pH response. Several possible reasons for this observation are explored. It is suggested, and density functional theory (DFT) calculations support, that the relative π* levels of the pH sensitive and the accessory ligands are critical.

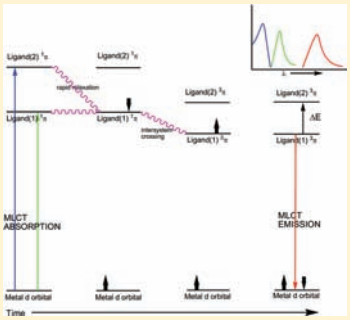

INTRODUCTION

The environmental sensitivity of many luminescent transition metal complexes has stimulated considerable effort to understand the origins of these effects. Attempts to obtain both a fundamental understanding and to harness the effects to create dyes which are useful in sensor applications are widely reported.[1] One of the more salutary aspects of these complexes is the ability to subtly modify their structure to elicit useful changes in photophysical behavior.[2] Gross changes can be obtained by changing the central metal ion, but finer changes can be obtained by modest alterations in the ligands. Thus, one can modify the lifetime, emission maxima, and emission intensity by suitable structural changes to the ligands of the complex.[3] Unfortunately, such tuning is still as much art as science.

We have been involved in attempting to understand how relatively small structural changes alter the environmental sensitivity and photophysical properties of complexes whose lowest excited state derives from a metal-to-ligand charge-transfer (MLCT) transition. The environmental driver is pH,[4] and central metal ions have included Re(I), Ru(II), and Os(II).[5] These ions offer the opportunity to create mixed ligand, or heterolepic complexes in which the environmentally sensitive ligand is partnered with other accessory ligands which may alter the photophysical response in useful ways. In this report we examine the role of the accessory ligand in pH sensitive Ru(II) complexes. Because the analyte detection step is quite simple and well understood we can focus cleanly on the role of the accessory ligand. The degree to which these accessory ligands can impact the response of the complex to its environment is, by comparison, little studied.[6]

Our simple starting point was that the impact of the accessory ligands would relate to the degree to which the various ligand π* orbitals mixed in the emitting electronic state of the complexes. By selecting accessory ligands with known useful effects on the emission, we hoped to enhance the response of the core molecular reporter. To some degree this hope was realized, but we also discovered unexpected pitfalls.

We chose Ru(II) as the central metal atom and 5-diethylamino-1,10-phenanthroline (5-Et_2Nphen) as the environmentally sensitive ligand. We then systematically changed the accessory ligands guided by the prior work on the impact of various ring substitutions on the photophysical properties of the respective tris complexes of the accessory ligands. As is often the case, our successes actually generated both answers and more questions.

EXPERIMENTAL SECTION

General Information and Materials. Except as noted, all chemicals were obtained from Sigma-Aldrich and used without further purification. The $Ru(III)Cl_3$*·xH_2O was obtained from Johnson Matthey Co. cis-Ru(2,2′ bipyridine)$_2Cl_2$*·$2H_2O$ was purchased from Strem Chemical Co. The ligands 1,10-phenanthroline (phen), 5-chloro-1,10 phenanthroline (5-Clphen), 4, 7-dimethyl-1,10-phenanthroline(Me_2phen), 3,4,7,8-tetramethyl-1,10-phenanthroline-(Me_4phen), 4,7-diphenyl-1,10-phenanthroline(φ_2-phen), 2,2′-bipyridine(bpy), 4,4′-dimethyl-2,2′-bipyridine(Me_2bpy), and 4,4′-diphenyl-2,2′-bipyridine(φ_2-bpy) were purchased from GFS Chemical.

Instrumentation. NMR spectra were obtained using a Bruker ERX 400 MHz instrument. UV−visible spectra were obtained with a

Received: May 25, 2011
Published: March 6, 2012

   dx.doi.org/10.1021/ic201114u | *Inorg. Chem.* 2012, 51, 3355−3365

Shimadzu UV-1601 spectrometer. Corrected room and low temperature emission spectra were obtained using a Spex FluoroMax instrument. Low temperature, 77 K, emission spectra were obtained using CH_3OH/C_2H_5OH (1:4) as a glassing solvent. IR spectra were recorded on a Midac FT-IR instrument. Lifetime measurements were made using a locally constructed apparatus utilizing an LSI -VSL nitrogen laser (λ = 337 nm, 3 ns pulse width) as the excitation source. The decay curves were averages of 100 individual decays and analyzed using a Marquardt based nonlinear least-squares fitting routine. Quantum yields were based on the accepted value of 0.042 for $Ru(bpy)_3Cl_2$ in degassed water[7] and the appropriate refractive index corrections were applied.

Structure and purity were verified by ^{1}H NMR, high resolution mass spectra, elemental analysis, and UV−vis spectra. Elemental analyses were done by Atlantic Microlabs, Norcross, GA, while mass spectral analyses were performed by the Mass Spectrometer Facility, Chemistry Department, North Carolina State University, Raleigh, NC. Assignments for ^{1}H NMR spectra were facilitated by model complex spectra using 5-methyl-1,10 phenanthroline as the proxy for the 5-diethylamino-1,10 phenanthroline. The model complexes were synthesized using unambiguous routes. For complexes with multiple isomers and broken symmetry, an unambiguous ^{1}H NMR assignment could not be made. All complexes were purified by column chromatography and gave materials for which thin layer chromatography (TLC) showed only one spot with two different solvent systems. Emission purity was established by lifetime measurements, that is, a single lifetime in CH_3OH, and an acceptable excitation spectra ratio which was flat to within 2%.[8]

Electrochemical measurements of the first reduction potential for $[Ru(5\text{-}Et_2Nphen)_3]^{2+}$ and $[Ru(4,7\text{-}Cl_2phen)_3]^{2+}$ were made using a BAS Model CV-1B potentiostat with a Ag/AgCl reference electrode and a glassy carbon working electrode. The measurements were done in dried CH_3CN with 0.1 M Bu_4NClO_4 (recrystallized) as added electrolyte. Ferrocene was used as an internal standard. At scan rates of 50 mV/s the waves were reversible.

Ligands and Complexes. Figure 1 shows the basic core complex where L = the accessory ligand. All the complexes were prepared by adapting well-known literature preparations[9] as described below.

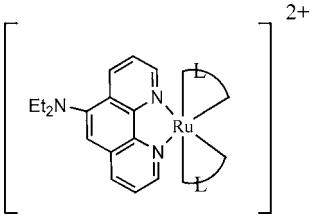

Figure 1. Basic Core Complex (L = Accessory Ligand).

Ligands. *5-Diethylamino-1,10-phenanthroline.* The pH sensitive ligand was prepared in three steps using an extension of the work of Kishnan[10a] and Shen.[10b]

To a rapidly stirred mixture of 450 mL of commercial Chlorox, 300 mL of water, 1.25 g of tetrabutylammonium hydrogen sulfate, and 250 mL of CH_2Cl_2 at 20 °C was added 2.5 g of 1,10-phenanthroline monohydrate (12.6 mmol). During the 3 h reaction time the pH was maintained at 8.5−8.6, and the temperature maintained at 20 ± 1 °C. At the end of the reaction, the CH_2Cl_2 layer was separated, and its volume reduced to ∼30 mL. Acetone was added until the formation of the white precipitate was complete. The 5,6-epoxy-1,10 phenanthroline was collected via suction filtration and dried in air. Gas chromatography showed this product >97% pure and thus adequate for the next step. Yields were ∼50%. ^{1}H NMR(400 MHz, $CDCl_3$): δ/ppm 4.62(s, 2H), 7.44(dd, J = 4.6, 7.9 Hz, 2H), 8.00(dd, J = 2.0, 7.8 Hz, 2H), 8.91(dd, J = 2.0, 4.6 Hz, 2H).

Next, 1.0 g (5.1 mmol) of the epoxide, 5 mL (3.54 g, 48 mmol) of diethylamine, and 10 mL of DMF were refluxed for 6 h. The solvent was removed, and the material, 5-diethylamino, 6-hydroxy-5,6-dihydro-1,10-phenanthroline used for the next step. Gas chromatography showed a single product, but this intermediate was not characterized.

Then 0.5 g of 5-diethylamino, 6-hydroxy-5,6-dihydro-1,10-phenanthroline (1.86 mmol) was dissolved in dry, refluxing 1,4-dioxane. To this was added in 3 portions, 1 g of NaH (60% in mineral oil) (25 mmol, 12 X excess) over 20 min. This mixture was refluxed for 4 h, and the reaction terminated by careful addition of 95% ethanol. The solvent was removed, and the dark waxy product washed with hexane. The product was dissolved in CH_2Cl_2, washed with water, and dried over anhydrous $MgSO_4$. The light tan material was shown by gas chromatography to be >98% pure. ^{1}H NMR spectra and elemental analysis confirmed the desired product. Typical overall yields were 40% based on starting 1,10 phenanthroline. The major loss occurs in the initial epoxidation step.

^{1}H NMR(400 MHz, $CDCl_3$): δ 0.99 (t, J = 7.0 Hz, 6H), 3.15 (q, J = 7.0 Hz, 4H), 7.16 (s, 1H), 7.42 (dd, J = 4.5 Hz, 1H), 7.50 (dd, J = 4.3 Hz, 1H), 7.99 (dd, J = 1.8 Hz, 1H), 8.56 (dd, J = 1.8 Hz, 1H), 8.94 (dd, J = 1.5 Hz, 1H), 9.05 (dd, J = 1.8 Hz, 1H). Anal. Calcd for $C_{16}H_{17}N_3$: C, 76.45; H, 6.84; N, 16.71. Found: C, 76.55; H, 6.93; N, 16.52.

4,7-Dichloro-1,10 phenanthroline (4,7-Cl_2phen). This preparation followed the procedures of Snyder and Freier.[11] The final product was characterized by ^{1}H NMR and elemental analysis.

^{1}H NMR(400 MHz, $CDCl_3$): δ 7.66(d, J = 4.4 Hz, 2H), 8.12 (s, 2H), 8.81(d, J = 4.4 Hz, 2H). Anal. Calcd for $C_{12}H_6N_2Cl_2$: C, 57.86; H, 2.43; N, 11.26. Found: C, 57.75; H, 2.36; N, 11.30.

Complexes. *Preparation of RuL_2Cl_2 Intermediates.* The heteroleptic complexes RuN_1−RuN_3 and RuN_5−RuN_7 were synthesized by first preparing the appropriate cis-Ru(II)L_2Cl_2 complex where L is the accessory ligand. These intermediates were prepared using a modification of the procedure reported by Meyer.[9a]

Typically 100 mg (0.416 mmol) of $RuCl_3$*H_2O, 2 equiv (0.832 mmol) of the accessory ligand, and 0.5 g of LiCl were refluxed in 5 mL of DMF for 3 to 6 h. The reactions were followed by TLC (alumina plates with CH_2Cl_2/CH_3CN (80:20) eluant). After the requisite reaction time, the solvent volume was reduced, and a small amount of water was added to the residue. This slush was filtered and washed with water and diethylether. The dark amorphous solid was dried, dissolved in CH_2Cl_2 and placed on a neutral alumina column. Elution with CH_2Cl_2 containing increasing amounts of CH_3CN served to isolate the desired dark maroon intermediate. Authentication was by UV−vis with a strong MLCT band in the 500 nm range. Yields ranged from 50 to 70%.

The synthesis of $Ru(5\text{-}Et_2Nphen)_2Cl_2$ for RuN_7 was more challenging as this ligand was readily oxidized by the Ru(III) at DMF reflux temperature, a common problem for functionalized ligands.[12] For this complex, 100 mg of $RuCl_3$*H_2O (0.416 mmol) and 0.5 g LiCl were placed in a microwave tube with ∼3 mL of 95% ethanol. The brown mixture was irradiated with 100 W for 5 min at 110 °C (CEM Discover system). To the resulting forest green solution was added 209 mg (0.832 mmol) of 5-Et_2Nphen, and the mixture was refluxed for 2 h. The reaction was followed by TLC (alumina plates with CH_2Cl_2/CH_3CN (80:20) eluant). The reaction was stopped after complete disappearance of the ligand. The reaction mixture contained the tris complex, identified by its luminescence, the desired bis complex (maroon color), and an additional complex which did not move on the alumina plate. Solvent removal, followed by treatment with aliquots of CH_2Cl_2 gave a dark maroon solution. The undissolved solid, mostly LiCl, was removed by filtration, and the solution placed on a short column of neutral alumina. Elution with CH_2Cl_2 and increasing amounts of CH_3CN separated the various factions and allowed isolation of the $Ru(5\text{-}Et_2Nphen)_2Cl_2$. The yields were only fair (∼ 25%).

The $[Ru(5\text{-}Et_2Nphen)_3]Cl_2$ was also collected from the column and converted to the perchlorate salt as outlined below.

[Ru(5-Et_2Nphen)L_2](ClO_4)$_2$; Method 1. This method was used for RuN_1−RuN3, RuN_5 and RuN_6. A 100 mg portion of the

dx.doi.org/10.1021/ic201114u | Inorg. Chem. 2012, 51, 3355−3365

appropriate RuL_2Cl_2 intermediate and a 50% molar excess of 5-Et_2Nphen were refluxed in 4:1 ethanol:water solvent until TLC-(alumina plates with CH_2Cl_2/CH_3CN (80:20) eluant) showed complete conversion of the intermediate; usually 3 to 5 h. Dropwise addition of this reaction mixture to a hot, stirred solution of saturated $LiClO_4$ was followed by removal of the ethanol via an N_2 stream. The mixture was cooled in an ice/water bath, and the resulting precipitated perchlorate complex was isolated by suction filtration and washed with cold water. The crude complex was dried at 65 °C and then dissolved in either acetone or CH_2Cl_2. The complex solution was placed on a neutral alumina column and eluted with either acetone or CH_2Cl_2 containing 4% CH_3OH and 1% triethylamine. The desired fraction was collected, concentrated and then added dropwise to a rapidly stirred beaker of chilled diethylether. The resulting orange solid was then collected via suction filtration. Yields ranged from 70−90%.

Warning! *Perchlorates are potentially explosive and should be handled with great care! Do not heat to dryness and use small amounts.*

[Ru(5-Et$_2$Nphen)L$_2$](ClO$_4$)$_2$; Method 2. For the complexes RuN_8 and RuN_11−13, the intermediate Ru(5-Et_2Nphen)$(DMSO)_2Cl_2$ was first prepared following a procedure similar to that of Wilkinson.[9d] A 200 mg portion of $RuCl_3$*H_2O (0.832 mmol) was refluxed for 10 min in 5 mL of dimethylsulfoxide. The solvent volume was reduced and acetone added resulting in a copious precipitate of yellow/green solid. The solid $Ru(DMSO)_4Cl_2$ was collected and washed with acetone and diethylether. Mp 192−194 °C (decomp). Yield ∼70%.

A 100 mg portion of $Ru(DMSO)_4Cl_2$ (0.206 mmol) and 52 mg (0.206 mmol) of 5-Et_2Nphen were refluxed in 5 mL of DMF for 15 min. The solvent was removed, and the reaction product dissolved in 15 mL of 95% ethanol. To this was added a 50% molar excess (0.618 mmol) of the appropriate accessory ligand, and the mixture refluxed for 5 h. The reaction mixture was then added dropwise to a stirred saturated solution of $LiClO_4$ and treated as in Method 1.

Ru(5-Et$_2$Nphen)$_2$(CN)$_2$. To 100 mg (0.148 mmol) of Ru(5-Et_2Nphen$)_2Cl_2$ dissolved in 30 mL of dry tetrahydrofuran (THF) was added 31 mg (0.148 mmol) of anhydrous $AgClO_4$. This mixture was stirred at 50 °C for 3 h, cooled, and the AgCl precipitate was removed via suction filtration. To the solution was added 200 mg of (4.1 mmol, 27 X excess) NaCN dissolved in a minimum amount of water. This mixture was refluxed for 4 h, cooled, and the solvent removed. To the solid was added both water and CH_2Cl_2 and stirred until complete dissolution. The CH_2Cl_2 layer was separated, washed twice with water, dried over anhydrous $MgSO_4$, and the solvent removed. The resulting orange/red solid was purified by column chromatography using neutral alumina with CH_2Cl_2/CH_3CN mixtures as the eluant. Yields were ∼50%.

Individual Complexes. *[Ru(5-Et$_2$Nphen)(bpy)$_2$](ClO$_4$)$_2$.* (RuN_1). ^{1}H NMR (400 MHz, CD_3CN): δ 1.15(t, J = 7.0 Hz, 6H), 3.38(q, J = 7.0 Hz, 4H), 7.24(t, J = 7.0 Hz, 2H), 7.43(m, 2H), 7.56(d, J = 5.3 Hz, 2H), 7.60(q, J = 3.0 Hz, 1H), 7.61(s, 1H), 7.68(q, J = 3.3 Hz, 1H), 7.82−7.87(m, 3H), 7.96−8.03(m, 3H), 8.06−8.10(m, 2H), 8.40(dd, J = 1.3 Hz, 1H), 8.49(d, J = 8.0 Hz, 2H), 8.52(dd, J = 1.3 Hz, 2H), 8.72(dd, J = 1.3 Hz, 1H). ESI-MS (m/z): (M^+), $C_{36}H_{33}N_7Ru$, Expected = 665.1841, Found = 665.1850. Anal. Cal.(%)for $C_{36}H_{33}N_7O_8Cl_2Ru$*-H_2O: C = 49.09, H = 3.99, N = 11.11. Found(%): C = 48.78, H = 4.10, N = 10.95.

[Ru(5-Et$_2$Nphen)(Me$_2$bpy)$_2$](ClO$_4$)$_2$. (RuN_2). ^{1}H NMR (400 MHz, CD_3CN): δ 1.18(t, J = 7.0 Hz, 6H), 2.51(d, J = 3.0 Hz, 6H), 2.60(s, 6H), 3.44(q, J = 7.0 Hz, 4H), 7.21(dd, J = 7.5 Hz, 2H), 7.44(d, J = 5.8 Hz, 2H), 7.65(dd, J = 1.8 Hz, 2H), 7.79(q, J = 5.3 Hz, 1H), 7.85(s, 1H), 7.88−7.95(m, 3H), 8.18(d, J = 5.0 Hz, 1H), 8.37(d, J = 5.3 Hz, 1H), 8.60(d, J = 8.3 Hz, 1H), 8.69(s, 2H), 8.74(s, 2H), 8.83(d, J = 8.3 Hz, 1H). ESI-MS (m/z): (M^+), $C_{40}H_{41}N_7Ru$, Expected = 721.2467, Found = 721.2462 . Anal. Cal(%) for $C_{40}H_{41}N_7O_8Cl_2Ru$*-H_2O: C = 51.20, H = 4.62, N = 10.45. Found(%): C = 51.46, H = 4.60, N = 10.44.

[Ru(5-Et$_2$Nphen)(phen)$_2$](ClO$_4$)$_2$. (RuN_3). ^{1}H NMR (400 MHz, CD_3CN): δ 1.26(t, J = 7.3 Hz, 6H), 3.04(q, J = 7.3 Hz, 4H), 7.49(q, J = 5.3 Hz, 1H), 7.56−7.67(m, 6H), 7.81(dd, J = 1.3 Hz, 1H), 7.97(dd, J = 1.0 Hz, 1H), 7.99−8.03(m, 2H), 8.05−8.08(m, 2H), 8.24(s, 4H), 8.39(dd, J = 1.3 Hz, 1H), 8.57−8.61(m, 4H), 8.70(dd, J = 1.3 Hz, 1H). ESI-MS (m/z): (M^+/2), $C_{40}H_{33}N_7Ru$, Expected = 356.5920, Found = 356.5912. Anal. Cal.(%) for $C_{40}H_{33}N_7O_8Cl_2Ru$*$2H_2O$: C = 50.69, H = 3.93, N = 10.34. Found(%): C = 50.43, H = 3.90, N = 10.45.

[Ru(5-Et$_2$Nphen)$_3$](ClO$_4$)$_2$. (RuN_4). ^{1}H NMR.(Mixture of geometric isomers). ESI-MS (m/z): (M^+/2), $C_{48}H_{51}N_9Ru$, Expected = 427.6657, Found = 427.6647. Anal. Cal(%) for $C_{48}H_{51}N_9$-O_8Cl_2Ru*$2H_2O$: C = 52.89, H = 5.08, N = 11.56. Found(%): C = 53.01, H = 4.98, N = 11. 48.

[Ru(5-Et$_2$Nphen)(Me$_4$phen)$_2$](ClO$_4$)$_2$. (RuN_5). ^{1}H NMR (400 MHz, CD_3CN): δ 1.15(t, J = 7.0 Hz, 6H), 2.22(m, 12H), 2.75(m, 12H), 3.38(q, J = 7.0 Hz, 4H), 7.46(q, J = 5.0 Hz, 1H), 7.55(q, J = 5.3 Hz, 1H), 7.67(s, 1H), 7.70−7.76(m, 5H), 7.92(dd, J = 1.3 Hz, 1H), 8.33−8.35(dd, J = 1.3 Hz, 5H), 8.66(dd, J = 1.2 Hz, 1H). ESI-MS (m/z): (M^+/2), $C_{48}H_{49}N_7Ru$, Expected = 427.6657, Found = 427.6647. Anal. Cal(%) for $C_{48}H_{49}N_7O_8Cl_2Ru$*$2H_2O$: C = 54.39, H = 5.04, N = 9.24. Found(%): C = 54.58, H = 5.00, N = 9.12.

[Ru(5-Et$_2$Nphen)(Me$_2$phen)$_2$](ClO$_4$)$_2$. (RuN_6). ^{1}H NMR(400 MHz, CD_3CN): δ 1.18(t, J = 7.0 Hz, 6H), 2.91(d, J = 2.5 Hz, 12H), 3.41(q, J = 6.8 Hz, 4H), 7.46−7.52(m, 5H), 7.58(q, J = 5.3 Hz, 1H), 7.67(s, 1H), 7.82−7.92(m, 5 H), 7.99(dd, J = 1.3 Hz, 1H), 8.37−8.40(m, 5H), 8.70(dd, J = 1.2 Hz, 1H). ESI-MS (m/z): (M^+/2), $C_{44}H_{41}N_7Ru$, Expected = 384.6244, Found = 384.6249. Anal. Cal(%) for $C_{44}H_{41}N_7O_8Cl_2Ru$*H_2O: C = 53.60, H = 4.40, N = 9.94. Found(%): C = 53.48, H = 4.36, N = 10.05.

[Ru(5-Et$_2$Nphen)$_2$](CN)$_2$. (RuN_7). ^{1}H NMR (Mixture of geometric isomers). ESI-MS (m/z): $(M+H)^+$, $C_{34}H_{35}N_8Ru$, Expected 656.2032, Found = 656.2031. Anal. Cal(%) for $C_{34}H_{34}N_8Ru$*$2H_2O$: C = 59.03, H = 5.53, N = 16.19. Found(%): C = 58.85, H = 5.56, N = 16.13.

[Ru(5-Et$_2$Nphen)(4,7-Cl$_2$phen)$_2$](ClO$_4$)$_2$. (RuN_8). ^{1}H NMR(400 MHz, CD_3CN):δ 1.14(t, J = 8.5 Hz, 6H), 3.48(q, J = 8.4 Hz, 4H), 7.47(dd, J = 4.7, 5.2 Hz, 1H), 7.54(dd, J = 4.7, 5.2 Hz, 1H), 7.62(s, 1H), 7.71−7.74(m, 4H), 7.80(d, J = 5.2 Hz, 1H), 7.91−7.99(m, 5H), 8.37(d, J = 7.8 Hz, 1H), 8.55(s, 4H), 8.68(d, J = 8.4 Hz, 1H). ESI-MS (m/z): $(M+H)^+$, $C_{40}H_{30}N_7Cl_4Ru$, Expected 850.0360, Found = 850.0352. Anal. Cal(%) for $C_{40}H_{29}N_7O_8Cl_6$ Ru*H_2O: C = 45.01, H = 2.93, N = 9.18. Found(%): C = 45.10, H = 2.84, N = 9.05.

[Ru(5-Et$_2$Nphen)(φ_2-phen)$_2$](ClO$_4$)$_2$. (RuN_11). ^{1}H NMR(400 MHz, CD_3CN): δ 1.18(t, J = 7.0 Hz, 6H), 3.41(q, J = 7.0 Hz, 4H), 7.57−7.70(m, 26H), 7.67(s, 1H), 7.99(d, 5.3 Hz, 1H), 8.11−8.15(m, 3H), 8.16(d, 1.8 Hz, 4H), 8.22(dd, 5.6, 5.5 Hz, 2H), 8.44(d, 8.6 Hz, 1H), 8.76(d, 8.5 Hz, 1H). ESI-MS (m/z): $(M+H)^+$/2 $C_{64}H_{50}N_7Ru$, Expected = 509.1585, Found = 509.1582. Anal. Cal(%) for $C_{64}H_{49}N_7$-O_8Cl_2Ru*H_2O: C = 62.28, H = 4.16, N = 7.94. Found(%): C = 62.52, H = 4.11, N = 8.13.

[Ru(5-Et$_2$Nphen)(5-Clphen)$_2$](ClO$_4$)$_2$. (RuN_12). ^{1}H NMR (Mixture of geometric isomers). ESI-MS (m/z): $(M+H)^+$ $C_{40}H_{32}N_7Cl_2Ru$, Expected = 782.1140, Found = 782.1147 . Anal. Cal(%) for $C_{40}H_{31}N_7$-O_8Cl_4Ru*H_2O: C = 48.11, H = 3.52, N = 9.81. Found(%): C = 47.89, H = 3.21, N = 9.71.

[Ru(5-Et$_2$Nphen)(φ_2-bpy)$_2$](ClO$_4$)$_2$. (RuN_13). ^{1}H NMR(400 MHz, CD_3CN): δ 1.16(t, 7.0 Hz, 6H), 3.38(q, 7.2 Hz, 4H), 7.38−7.51(m, 11H), 7.60(dd, 5.8 Hz, 2H), 7.72−7.89(m, 12H), 8.06(d, 5.8 Hz, 2H), 8.12(d, 5.8 Hz, 1H), 8.15(d, 5.8 Hz, 2H), 8.26(d, 7.5 Hz, 1H), 8.35(d, 5.0 Hz, 1H), 8.57(s, 2H), 8.61(d, 5.0 Hz, 4H), 8.67(d, 8.4 Hz, 1H). ESI-MS (m/z): $(M+H)^+$/2 $C_{60}H_{50}N_7Ru$, Expected = 485.1586, Found = 485.1583. Anal. Cal(%) for $C_{60}H_{49}N_7O_8Cl_2Ru$: C = 61.70, H = 4.23, N = 8.38. Found(%): C = 61.71, H = 4.21, N = 7.92.

pH Titrations. Stock aqueous solutions of the various complexes were made by stirring ∼100 mL of deionized water with an excess of the appropriate complex for about 4 h at room temperature. The solution was filtered through a Gelman 0.45 μ Acrodisc. The filtered stock served as the basis for both intensity and lifetime measurements.

The buffer solutions used employed H_3PO_4, KH_2PO_4, K_2HPO_4, and K_3PO_4 in varying proportions. The buffer concentration was 0.1 M. The pH of the buffers was determined using a Corning Model 440 pH meter. Typically, 1 mL of the stock solution of complex and 3 mL of buffer were combined for the intensity or lifetime measurement. There was no detectable pH difference between the pure buffer solution and

dx.doi.org/10.1021/ic201114u | Inorg. Chem. 2012, 51, 3355−3365

the test solution. The luminescence intensity and lifetime measurements were made with air-saturated solutions.

Buffered solution lifetimes for all complexes, except RuN_7 at pH < 3.5, were satisfactorily fit by a single exponential. The lifetime for RuN_7 was evaluated as a mean lifetime using eq 1.

$$\tau_M = \sum(A_i\tau_i^2/\sum A_j\tau_j) \quad (1)$$

Here A_i and τ_i are the pre-exponential and lifetime for the i-th component. $\sum A_j\tau_j$ is the sum of the pre-exponential-lifetime product terms. Only 2 exponentials were required for satisfactory fit. The necessity of multiple terms is attributed to the onset of protonation of the CN ligands.[13]

To test specific ion effects, a limited number of both intensity and lifetime titrations were also done using a buffer system based on H_2SO_4, $KHSO_4$, and K_2SO_4. This buffer yielded results indistinguishable from the phosphate buffer system. Tests were also run to ensure the complexes were stable at low pH for the duration of our measurements (Supporting Information, Figure S1).

Data Fitting/Analysis. Except as noted above, all the luminescence decays observed in this study were satisfactorily fitted with a single exponential decay with no evidence of a second component. At the high buffer concentrations used this is not unexpected and is consistent with the rapid exchange limit. In the fast exchange limit, it is assumed that the excited state equilibrium between HA* and A^{-}* is maintained. Under these conditions only a single decay is seen, characterized by a single observed lifetime, τ_{obs}, which implies a single observed decay rate constant k_{obs}. Using Scheme 1, this

Scheme 1. Protonation Equilibrium for Ground and Excited States

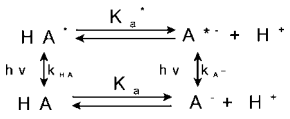

allows for very simple expressions for the observed intensity and lifetime variations as a function of the fraction of each species present.[14]

$$\text{Intensity:} \quad I_{obs} = f_{HA}I_{HA}^{max} + f_A I_A^{max} \quad (2)$$

$$\text{Lifetime:} \quad k_{obs} = f_{HA}k_{HA} + f_A k_A \quad (3)$$

Here f_{HA} and f_A are the fractions of HA* and A^{-}* present, respectively, I^{max} is the emission intensity when only that species is present, and k_{HA} and k_A are the decay rate constants for the HA* and A^{-}* species. The fraction of each species present will depend on the pH and pK_a* of the excited state of the complex. When this dependence is incorporated into eqs 2 and 3, one obtains

$$I_{obs} = (1 + 10^{(pH-pKa^*)})^{-1} \times I_{HA}^{max} + [1 - (1 + 10^{(pH-pKa^*)})^{-1}] \times I_A^{max} \quad (4)$$

$$k_{obs} = 1/\tau_{obs} = (1 + 10^{(pH-pKa^*)})^{-1} \times k_{HA} + [1 - (1 + 10^{(pH-pKa^*)})^{-1}] \times k_A \quad (5)$$

In the rapid exchange limit, these expressions are rigorously correct and make no assumptions regarding the excitation wavelength, only the limiting intensities or decay rates are required. Values for limiting I^{max} and k were obtained from the appropriate data at the limits of the pH range used where both the intensity and the lifetime had reached a constant value. Fitting the experimental data using a Marquardt approach required only a single floating parameter, pK_a*, the pK_a of the excited state. The fact that all decays except for RuN_7 at low pH could be fit with a single exponential suggests this simple model is adequate. The experimental data were fit with either eq 4 or 5 using PSI Plot software. The fits were all satisfactory, gave internally consistent values of pK_a* (i.e., intensity vs lifetime), and provided chemically reasonable values.

On the basis of absorption changes with pH (see Figure 2A), eq 4 was modified for use with absorbance and used to calculate the ground state pK_a for several of the complexes.

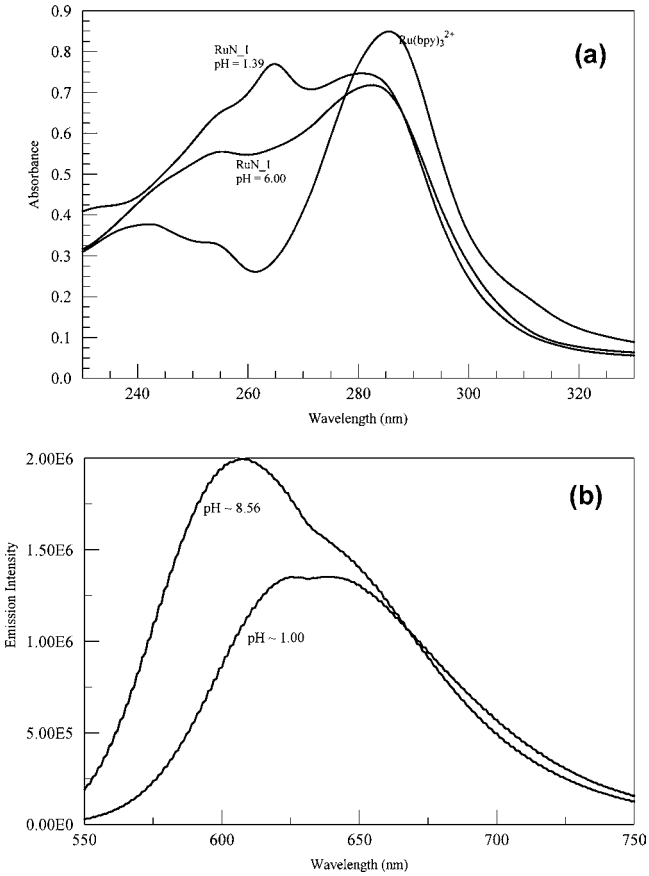

Figure 2. (a) Electronic absorbance spectra for $[Ru(5\text{-}Et_2Nphen)(bpy)_2]^{2+}$ at different pH in buffer solutions and $Ru(bpy)_3^{2+}$ in water. (b) Corrected emission spectra for $[Ru(5\text{-}Et_2N\ phen)(bpy)_2]^{2+}$ at high and low pH in buffer solutions.

Density Functional Theory (DFT) Calculations. We modeled the complex structures of RuN_1′ (simplified form of RuN_1 by replacement of Et with Me) and the 5-Clphen species, RuN-12, using Gaussian 09 software[15] for computations with the familiar B3LYP variant of the density functional,[16] using the Stuttgart–Dresden, SDD, basis[17] which includes a pseudopotential for the metal and reduces the number of electrons treated explicitly. For these large systems this modest basis still included up to 581 members for RuN_12. Counterions were not included in the modeling. Optimization of the structures of the complexes and calculations of spectra incorporated a Polarizable Continuum Medium model of the solvent[18] with the dielectric constant of water. Absorption spectra were estimated by TD-DFT[19] with the B3LYP density functional and the same SDD basis. The coordinates of the optimized geometries are provided in the Supporting Information.

RESULTS AND DISCUSSION

Table 1 shows basic photophysical properties of the complexes in CH_3OH. All complexes exhibit the expected MLCT absorption in the 450 nm region with ε values in line with similar complexes.[13] In addition to the MLCT band, the

dx.doi.org/10.1021/ic201114u | Inorg. Chem. 2012, 51, 3355–3365

Table 1. Photophysical Properties for $RuL'L_2$ Complexes in CH_3OH; L′ = 5-Et_2N-1,10-phenanthroline, L = Accessory Ligand

$[Ru(L')(L)_2]^{2+}$	Abs λ_{max} (nm)	ε (M^{-1} cm^{-1})[a]	Emis[b] λ_{max} (nm)	τ (μs)[c]	k_q (O_2) M^{-1} s^{-1}
$[Ru(L')(bpy)_2]$; RuN_1	453[d], 424,370	1.83×10^4	609	0.824	2.0×10^9
$[Ru(L')(Me_2bpy)_2]$; RuN_2	456[d], 426,350	2.33×10^4	609	1.06	3.2×10^9
$[Ru(L')(phen)_2]$; RuN_3	448[d], 421	1.52×10^4	597	1.45	3.8×10^9
$[Ru(5\text{-}Et_2Nphen)_3]$; RuN_4	456, 423, 369[d]	2.13×10^4	594	0.884	3.6×10^9
$[Ru(L')(Me_4phen)_2]$; RuN_5	423	2.08×10^4	612	1.58	4.4×10^9
$[Ru(L')(Me_2phen)_2]$; RuN_6	448, 425[d]	1.73×10^4	603	1.26	3.7×10^9
$[Ru(L')_2(CN)_2]$; RuN_7	457, 360[d]	1.03×10^4	631	1.40	3.0×10^9
$[Ru(L')(4,7\text{-}Cl_2phen)_2]$; RuN_8	448	2.44×10^4	632	2.02	3.7×10^9
$[Ru(L')(\varphi_2\text{-}phen)_2]$; RuN_11	459[d], 433	2.44×10^4	613	4.86	2.2×10^9
$[Ru(L')(5\text{-}Clphen)_2]$; RuN_12	450[d], 423	1.46×10^4	604	1.12	1.6×10^9
$[Ru(L')(\varphi_2\text{-}bpy)_2]$; RuN_13	471[d], 443	2.98×10^4	624	1.52	1.7×10^9

[a] ε for strongest peak. [b] Corrected. [c] Ar purged/CH_3OH. [d] Strongest peak.

complexes also exhibited near UV bands attributable to $\pi-\pi^*$ transitions of the ligands. The emissions were centered around 600 nm with a range of only about 40 nm among the various λ_{max} values. The lifetimes in purged CH_3OH, with the exception of RuN_11, were in the 1 to 2 μs range and showed only modest variation with changing spectator ligands. The emission is readily quenched by oxygen with quenching rates near the diffusion limit. This characteristic has an adverse impact on their use as sensors, though the lower solubility of O_2 in water, ~0.265 mM, ameliorates the problem to some degree.[20] Additionally, we have found that when the complexes are embedded in supports such as polymers, the quenching is further reduced.[21]

Figure 2A shows the impact of protonation on the UV spectra of $[Ru(5\text{-}Et_2Nphen)(bpy)_2](ClO_4)_2$. The spectrum of $[Ru(bpy)_3]Cl_2$ is also shown for comparison. The absorption between 250−270 nm is assigned to the 5-Et_2Nphen ligand on the basis of its singular absence in the model complex, $[Ru(bpy)_3]Cl_2$, and the pH dependence of this band. It is clear that protonation of the amine group causes a shift in the energy levels of the 5-Et_2Nphen ligand. This effect was used to determine the pK_a of the ground state for a representative sample of the complexes. The MLCT bands were also sensitive to pH, though not as dramatically as the near UV (Supporting Information, Figure S2). Qualitatively the relative change in absorbance with protonation tracks the dynamic range observed for the emission as a function of pH. Several of the complexes, RuN_8 and RuN_11−RuN_13, showed very muted luminescence response to pH, and their absorbance changes with pH in the 230−350 nm region were also virtually non existent.

Figure 2B shows the impact of protonation on the emission of the same complex, RuN_1. Protonation results in a red shift in λ_{max} and a decrease in the intensity of emission, consistent with reports for other nitrogen based pH sensitive Ru(II) complexes.[22] The actual change in the integrated emission is only ~35%, but by judicious choice of monitoring wavelength, the dynamic range, the ratio of single λ intensity at high and low pH, can be significantly improved. Most of the complexes gave useful pH-intensity response. This is illustrated in Figure 3 for RuN_1. Similar plots showed significant changes in the emission with pH for all complexes except RuN_8 and RuN_11−RuN_13. Table 2 summarizes the results.

Figure 4 shows a typical plot for the changes in emission lifetime with pH. The lifetime response to pH changes was very muted compared to that of the emission intensity. For none of the complexes was the dynamic range over 2, and many were nearly unresponsive. The small dynamic ranges encountered using lifetime measurements made the accurate determination of the pK_a* very difficult. For this set of complexes, using the lifetime as an indicator of pH is not useful.

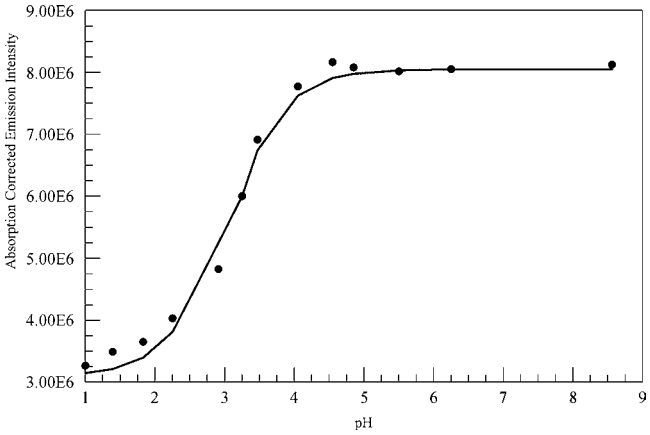

Figure 3. Emission intensity, corrected for both instrument response and absorbance, for $[Ru(5\text{-}Et_2Nphen)(bpy)_2]^{2+}$ as a function of pH in buffer solutions. Emission monitored at 595 nm.

Table 2. pK_a and Dynamic Ranges for Ru(II) Complexes

alias	complex	excited state pK_a	dynamic range	ground state pK_a
RuN_1	$[Ru(5\text{-}Et_2Nphen)(bpy)_2](ClO_4)_2$	3.1	2.4	1.8
RuN_2	$[Ru(5\text{-}Et_2Nphen)(Me_2bpy)_2](ClO_4)_2$	3.7	4.4	
RuN_3	$[Ru(5\ Et_2Nphen)(phen)_2](ClO_4)_2$	3.3	2.9	2.3
RuN_4	$[Ru(5\text{-}Et_2Nphen)_3](ClO_4)_2$	4.1	3.0	2.2
RuN_5	$[Ru(5\text{-}Et_2Nphen)(Me_4phen)_2](ClO_4)_2$	3.9	6.2	
RuN_6	$[Ru(5\text{-}Et_2Nphen)(Me_2phen)_2](ClO_4)_2$	3.8	1.9	
RuN_7	$[Ru(5\text{-}Et_2Nphen)_2](CN)_2$	4.5	3.5	2.9
RuN_8	$[Ru(5\text{-}Et_2Nphen)(4,7\text{-}Cl_2phen)_2](ClO_4)_2$	N.R.[a]	<1.3	
RuN_11	$[Ru(5\ Et_2Nphen)(\varphi_2\text{-}phen)_2](ClO_4)_2$	N.R.[a]	<1.3	
RuN_12	$[Ru(5\ Et_2Nphen)(5\text{-}Clphen)_2](ClO_4)_2$	N.R.[a]	<1.3	
RuN_13	$[Ru(5\ Et_2Nphen)(\varphi_2\text{-}bpy)_2](ClO_4)_2$	N.R.[a]	<1.3	

[a] N.R. = not pH responsive.

dx.doi.org/10.1021/ic201114u | Inorg. Chem. 2012, 51, 3355−3365

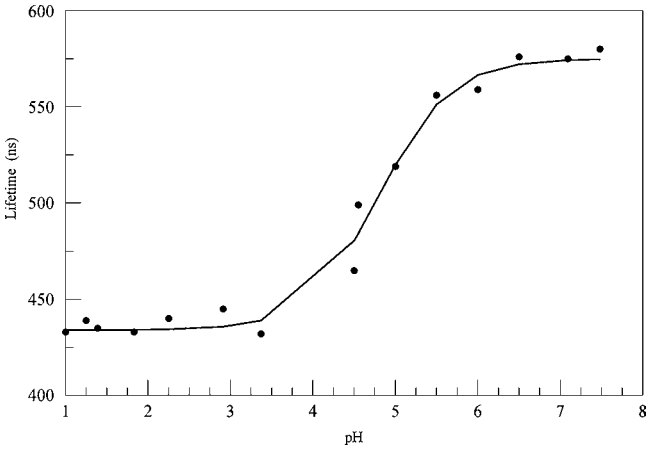

Figure 4. Emission lifetime as a function of pH for $[Ru(5\text{-}Et_2Nphen)(Me_4phen)_2]^{2+}$ in buffer solutions.

Using the Förster cycle to describe the relationship between the pK_a and pK_a^*, we expect

$$pK_a^* = pK_a + (0.625/T)(\nu_B - \nu_{HB}) \quad (6)$$

where $(\nu_B - \nu_{HB})$ is the difference between the emission of the neutral and protonated forms in wavenumbers (cm^{-1}).[23] Because the emitting state is ^{3}MLCT the emission data must be used. This relationship is well followed for these complexes. For example with RuN_1 the expected $(\nu_B - \nu_{HB})$ is 620 cm^{-1} versus an observed value of 612 cm^{-1}. This relatively good agreement suggests that protonation equilibrium is established in the excited state. When the fast exchange limit applies, one also expects

$$pK_a^* = pH_i + \log\ \tau_{HB}/\tau_B \quad (7)$$

where pH_i is the inflection point in the intensity versus pH titration curve. However, as the lifetimes of the two forms for these complexes differ by less than a factor of 2 under the most propitious conditions, the pK_a^* is effectively the pH_i.

The trends in pK_a^* values determined using the emission changes with pH are consistent with our earlier observations using complexes with 5-carboxy-1,10-phenanthroline as the pH sensitive element.[5] One major surprise, however, is the significant shift in the ground state pK_a when the free pH sensing ligand, 5-diethylamino-1,10-phenanthroline is complexed with Ru(II). We were not able to measure the pK_a of the free ligand directly, but the pK_a of *N*,*N*-diethylaniline should be a reasonable proxy. This aniline has a $pK_a \sim 6.6$.[24] While a shift to lower pK_a is expected because of the electron withdrawing power of the Lewis acid metal ion, our ground state pK_a measurements for these complexes fall in the range of ~2 to 3, which represents a shift of 4 orders of magnitude. As might be expected from the shift in electron density accompanying an MLCT excitation in which the transferred metal electron density is localized in the pH sensitive ligand, the pK_a^* of the excited states are about 1 to 2 orders of magnitude higher than the ground state values.[14a] Unfortunately, the excited state pK_a^* values are well below the optimal values necessary for both environmental and physiological monitoring.

The impact on the excited state pK_a^* of varying the accessory ligands is similar to our earlier study.[5] That is, if we take bpy or phen as the baseline for our accessory ligands, pendent methyl groups which are electron donating can raise the pK_a^* by as much as 0.5 units. If the formal charge on the Ru(II) is reduced by using a charged accessory ligand, as with RuN_7, the pK_a^* is incremented by >1 unit. However, a second surprise is that 5-Cl phen, 4,7-Cl_2phen, φ_2-phen, φ_2-bpy accessory ligands effectively mute the pH response of the complexes (Supporting Information, Figures S3A–S3D). The latter two accessory ligands were chosen because of the relatively high quantum yields of their tris complexes.[13] This finding forced us to reevaluate our simple localized excitation model of the excited state.

Ground State Mixing in Heteroleptic Ru(II) Complexes. In the simplest or decoupled picture of the MLCT electronic absorption process for a Ru(II) complex, an electron from a d orbital of the metal ion is transferred to one of the π^* ligand orbitals. This is a vertical transition with no spin change, resulting initially in a singlet excited state with a considerable change in the dipole moment of the complex. Elegant fast laser studies have revealed much about the temporal evolution of prototype complexes during the post-absorption time window.[25] These studies suggest that the final thermally equilibrated triplet emitting state is populated within a few picoseconds and that under some circumstances significant localization of the excitation can occur on a particular ligand. This is shown qualitatively as an evolving time diagram in Scheme 2. For tris complexes, the π^* energy levels of all the ligands are identical. The recent time-resolved absorption studies seem to point to significant excitation delocalization[25c] in contrast to earlier work which, on balance, seemed to favor localization.[26]

For heteroleptic complexes the picture is more complex in that the π^* orbitals of the various ligands are only rarely and accidentally the same energy. In this case, the simple decoupled model would suggest that the observed absorption spectrum would be the weighted sum of the allowed MLCT transitions associated with various component ligands.[27] If, however, there is some ground state mixing of the various ligand π^* orbitals, this simple approximation should give observably poor fits. This latter statement is somewhat arbitrary as the MLCT absorption for many tris Ru(II) complexes are not all that different.

Most of our complexes were of the type $RuL'L_2$, where L′ was the pH sensitive ligand 5-Et_2Nphen and the L's were common accessory ligands based on bpy or phen and their various ring substituted analogues. Absorption spectra were obtained in CH_3OH for RuL'_3^{2+}, our $RuL'L_2^{2+}$ complexes, and the related RuL_3^{2+} complexes. All the spectra were normalized to the same absorbance at the MLCT λ_{max}. The expected spectrum for the heteroleptic complex was then calculated as per $RuL'L_2^{2+} = (2 \times RuL_3^{2+} + RuL'_3^{2+})/3$. Because the normalization effectively removes the differences in molar extinction of the components, the final calculated spectra were scaled so that the calculated and actual heteroleptic spectra matched at λ_{max}. This involved multiplication by a constant that was never greater than ~1.07.

The two spectra, actual and calculated, for several of our heteroleptic complexes are shown in Figures 5A–5D. These include both our best and worst fits as well as two non pH responsive cases. Though our method is crude, the agreement is actually quite good and suggests that this simple, isolated chromophore model is a reasonable approximation for the absorption process. However, the failure to obtain exact fits may indicate some π^* or other state mixing even in the ground state for heteroleptic complexes in which the various π^* orbitals are not energetically widely separated.[28]

dx.doi.org/10.1021/ic201114u | *Inorg. Chem.* 2012, 51, 3355–3365

Scheme 2. Time Evolution of the Excited State after MLCT Absorption

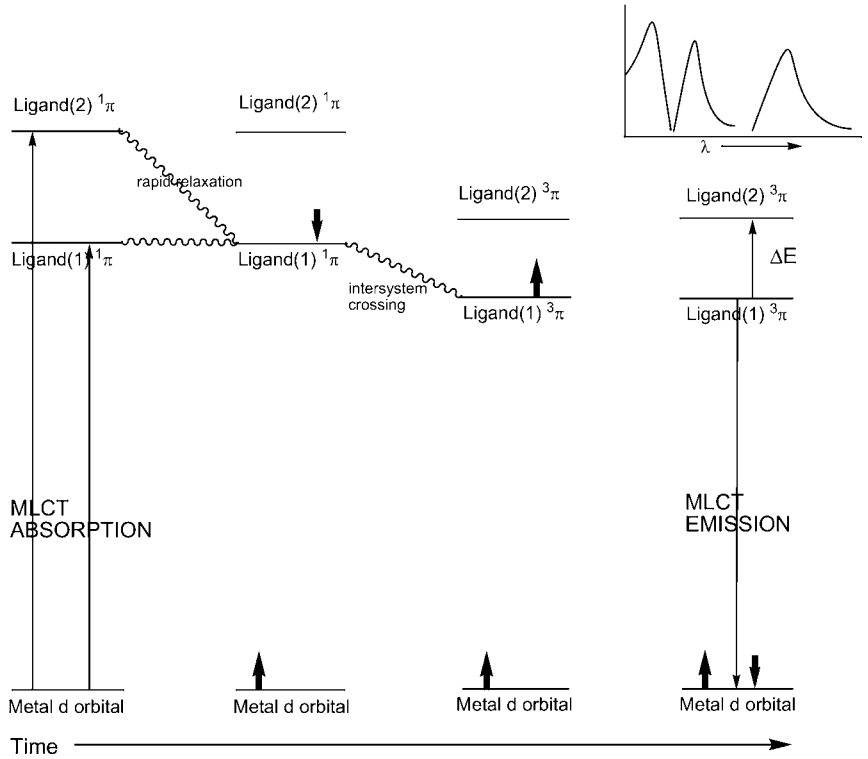

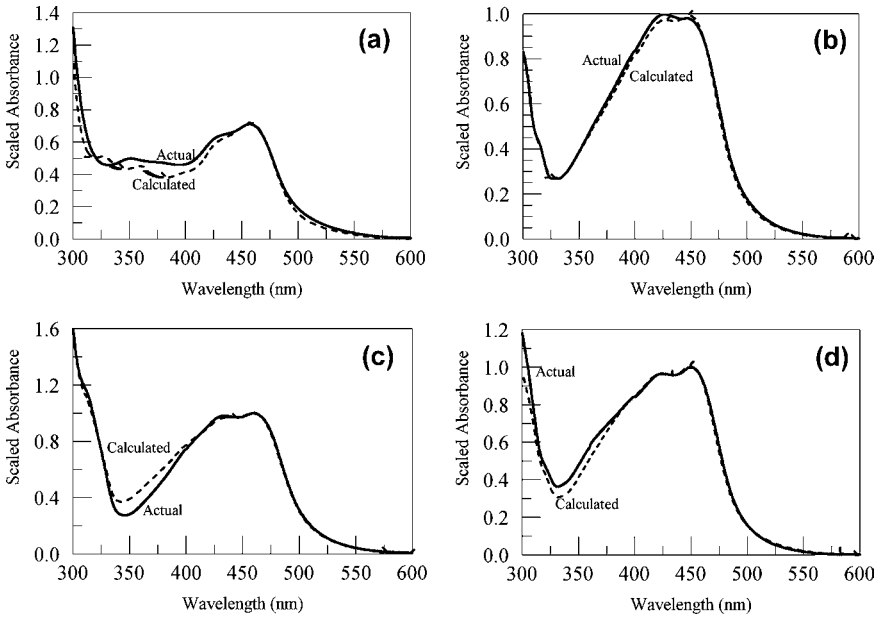

Figure 5. Comparison of actual and calculated electronic absorption spectra in CH_3OH for (a) $[Ru(5\text{-}Et_2Nphen)(Me_2bpy)_2]^{2+}$; (b) $[Ru(5\text{-}Et_2Nphen)(Me_2phen)_2]^{2+}$; (c) $[Ru(5\text{-}Et_2Nphen)(\varphi_2\text{-}phen)_2]^{2+}$; (d) $[Ru(5\text{-}Et_2Nphen)(5\text{-}Clphen)_2]^{2+}$.

Our approach to modeling the absorption spectra of these complexes using time-dependent DFT (TD-DFT) methods was limited to one-electron excitations that often underestimates excitation energies.[29] The complexity of the systems and limitations of our methods make the calculated spectra below 300 nm of lower reliability. We examined both a pH responsive (RuN_1′) and nonresponsive (RuN_12) complex and there was reasonable qualitative agreement between the calculated and observed spectra (Supporting Information). Features well captured by the calculations include the following: (1) General similarity of the form of the absorption spectra of all species; first absorption band (MLCT) located near 450 nm. (2) Noticeable intensity reduction was observed with protonation of the responsive species, while a lesser change was observed for the pH insensitive species. We also note that the frequently used orbital pictures were not particularly helpful in our effort to track the changes in electron density accompanying excitation.

Excited State Mixing and Its Impact on Environmental Sensitivity. The almost total lack (<10% intensity change,

dx.doi.org/10.1021/ic201114u | *Inorg. Chem.* 2012, 51, 3355−3365

< 7 nm λ_{max} emission shift) of pH sensitivity for the complexes $[Ru(5\text{-}Et_2Nphen)(\varphi_2\text{-phen})_2](ClO_4)_2$, $[Ru(5\text{-}Et_2Nphen)(5\text{-Cl phen})_2](ClO_4)_2$, $[Ru(5\text{-}Et_2Nphen)(4,7\text{-}Cl_2phen)_2](ClO_4)_2$, and $[Ru(5\text{-}Et_2Nphen)(\varphi_2\text{-bpy})_2](ClO_4$ was surprising. Remarkably, the φ_2-phen and φ_2-bpy complexes have the highest quantum yields and longest lifetimes of any of the suite.

On the basis of the localized excitation model (LEM), the emission originates from the lowest energy excited state and this state, for a heteroleptic complex, would involve the ligand with the lowest energy π^* orbital. If this ligand were the accessory ligand, L, then the environmental sensitivity of the complex would be muted unless protonation of the sensing ligand reversed the relative π^* energies. However, the fact that several complexes containing accessory ligands with lower energy π^* orbitals than the pH sensing ligand gave acceptable sensitivity suggested that this simple model may be inadequate.

Two modifications of the narrowly defined LEM can be suggested to address our experimental observations. The first retains the major features of the LEM but suggests that when the difference in the π^* energies of the two ligands, pH sensing and accessory, are not greatly different (i.e., < 500 cm^{-1}), then at room temperature there could be a substantial population in which the excitation is localized on the higher π^* energy ligand. For this model the response would be temperature dependent (TD-LEM).

A second model would invoke some measure of orbital mixing in the excited state in which the emission originates from an excited state of mixed orbital parentage (MOP). The amount of mixing between the sensing ligand and accessory ligand orbitals would depend, in part, on the relative energies of their respective π^* orbitals. The closer in energy, the greater the expected degree of mixing.

If the TD-LEM is correct, then at low temperature where thermal access to the higher π^* ligand is suppressed, the emissions from the heteroleptic complexes should very closely resemble those from the corresponding tris-complex with the lower π^* ligand.

We examined the emission for the prototype complex $[Ru(phen)_2(\varphi_2\text{-phen})]^{2+}$ at low temperature. The measured λ_{max} values for $Ru(phen)_3^{2+}$ and $Ru(\varphi_2\text{-phen})_3^{2+}$ complexes at 77 K in CH_3OH/C_2H_5OH glass are 17,700 cm^{-1} and 16,300 cm^{-1} respectively; $\Delta E \sim 1{,}400$ cm^{-1} . Assuming these values reflect the relative emitting state energies and are a proxy for the relative positions of the respective π^* orbitals, the probability of the emission involving a particular ligand assuming a simple exponential population dependence leads to a 6.25×10^{10} advantage for the emission involving the φ_2-phen ligand; neglecting any degeneracy terms. Thus, the low temperature emission spectrum for $[Ru(phen)_2(\varphi_2\text{-phen})]^{2+}$ should be quite similar to that of $[Ru(\varphi_2\text{-phen})_3]^{2+}$ based on the TD-LEM.

As Figure 6A clearly shows, the TD-LEM fails to predict the observed spectrum. We also tested this model using the pH sensing complex $[Ru(5\text{-}NH_2\ phen)(\varphi_2\text{-phen})_2]^{2+}$and comparing it with the respective tris-homoleptic complexes. As Figure 6B shows, the simple TD-LEM fails here as well. Inspection suggests that the emitting excited state must involve orbitals that are a mixture from both contributing ligands.

In Figure 6A, the effect of the φ_2-phen ligand is a modest red shift of the emission. The overall shape of the emission spectrum more closely resembles that of the tris-phen complex. The results of Figure 6B are quite similar, but the red shift is even greater because of the presence of 2 φ_2-phen ligands.

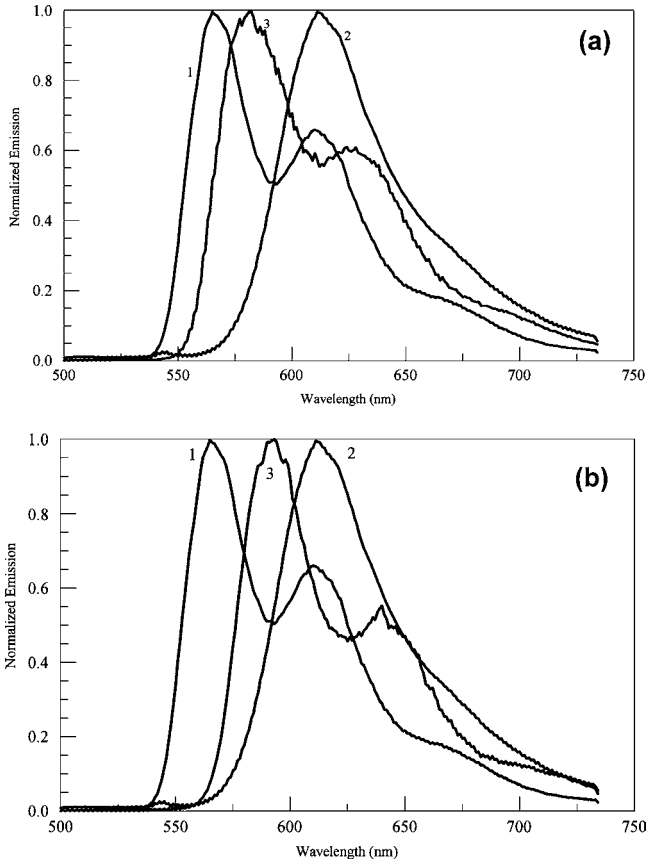

Figure 6. Comparison of corrected, normalized low temperature (77 K) emission spectra in CH_3OH/C_2H_5OH (1:4) (a): $[Ru(phen)_3]^{2+}$, (1); $[Ru(\varphi_2\text{-phen})_3]^{2+}$, (2); $[Ru(phen)_2(\varphi_2\text{-phen})]^{2+}$, (3). (b): $[Ru(phen)_3]^{2+}$, (1); $[Ru(\varphi_2\text{-phen})_3]^{2+}$, (2); $[Ru(5\text{-}Et_2Nphen)(\varphi_2\text{-phen})_2]^{2+}$, (3).

Again, the general features of the emission are those of the tris 5-Et_2Nphen complex.

As satisfying as these experiments are in suggesting that a mixed orbital excited state is present in our heteroleptic complexes, the actual situation is more complex. We examined the same cluster of complexes at room temperature, with startlingly different result. At the higher temperature, we would still expect emission from the φ_2-phen ligand to dominate according to the TD-LEM. However, the temperature dependence of the relative mixing of the π^* orbitals of the ligands is unknown. In addition, there may be solvent relaxation and conformational relaxations that affect this mixing. Further, the change from a rigid to fluid environment as well as different Franck−Condon factors due to higher temperature may significantly change the shapes of the emission envelopes.

As Figures 7A and 7B show, room temperature, fluid solution results in several changes. The entire spectra set are strongly red-shifted and much of the sharpness is lost. Also, the low temperature "phen" structure is lost, resulting in broad featureless peaks of nearly Gaussian shape. Remarkably, the spectra of the heteroleptic complexes are quite similar to the $[Ru(\varphi_2\text{-phen})_3]^{2+}$ complex in both shape and λ_{max}. Indeed, the spectral shift is only a few nm.

How can we interpret this? On the basis of a Boltzman distribution within the possible excited states, we expect the heteroleptic spectra to most closely resemble the lowest π^* tris complex at lower, not higher temperatures. Yet, the LEM now

dx.doi.org/10.1021/ic201114u | Inorg. Chem. 2012, 51, 3355−3365

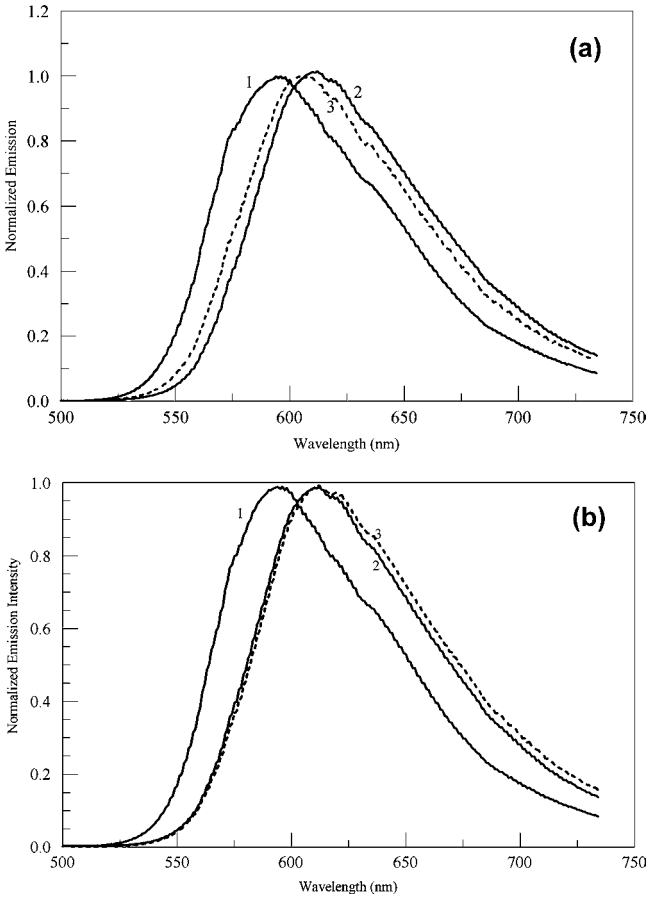

Figure 7. Comparison of corrected, normalized room temperature emission spectra in CH_3OH (a): $[Ru(phen)_3]^{2+}$, (1); $[Ru(\varphi_2\text{-phen})_3]^{2+}$, (2); $[Ru(phen)_2(\varphi_2\text{-phen})]^{2+}$, (3). (b): $[Ru(5\text{-}Et_2Nphen)_3]^{2+}$, (1); $[Ru(\varphi_2\text{-phen})_3]^{2+}$, (2); $[Ru(5\text{-}Et_2Nphen)(\varphi_2\text{-phen})_2]^{2+}$, (3).

appears to work as the emission strongly resembles that of the tris complex with the lower π^* ligand. The MOP model has many unknown parameters, but it is possible that the degree of mixing, in addition to dependence on the π^* energy separation, may change with environment and/or temperature. A clear choice among the various possible models is not possible from this limited data. However, it does seem that the situation for the emitting state(s) of these complexes is more complex than the "pure" LEM approach.

Seeking insight into the nature of the emitting state, we carried out a series of calculations. First, we estimated the energies of the π^* levels for some of our accessory ligands as well as a proxy for our pH sensitive ligand, again with the B3LYP/SSD model (see Supporting Information). While the calculations for the free ligands showed a significant difference between the π^* levels of the sensing and accessory ligands, there was no obvious distinction between the pH sensitive and pH muting accessory ligands. Thus, examining the π^* levels of the uncomplexed ligands was not particularly helpful.

We next modeled the emission which we assumed originated from the lowest triplet state; $E_{em} \sim E(T_1) - E(S_0')$, where $E(S_0')$ is the energy on the ground state singlet surface at the lowest-energy geometry of the triplet state. For the 5-chloro complex these energies are virtually identical for both unprotonated and protonated species, 1.733 and 1.730 eV, respectively. However, for the pH responsive system, RuN_1′, the vertical T-S gaps are 1.723 eV for the nonprotonated and 1.685 eV for the protonated complex. This corresponds to a vertical emission around 720 nm for the unprotonated and 737 nm for the protonated (Scheme 3). While, as expected, these

Scheme 3. Potential Energy Curves for Ground and First Excited States

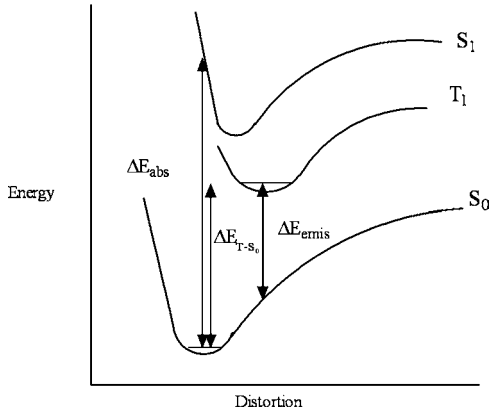

absolute emission energies are too low, the relative ordering results do support our observations that protonation should result in a red shift of tens of nanometers for the pH sensitive complexes and that the emission from the 5-Cl phen complex will have a smaller pH response.

We calculate the zero point energy differences between the S_0 and T_1 states would yield emission at 640 nm for the unprotonated RuN_1′ and 660 nm for the protonated species. We acknowledge that the energy differences predicted in these calculations are small and our methods are approximate. However, the calculations do support (1) a red emission shift on protonation, and (2) variation in pH sensitivity depending on the accessory ligand.

There is a rich literature, earlier work drawing largely from static and Resonance Raman measurements[26,30] and more recently fast kinetic studies,[25] which provides insight into the question of orbital mixing in Ru(II) heteroleptic complexes. The salient results suggest the following: (1) The first reduction potential for the appropriate tris complex is a good proxy for the energy of the ligand π^* state. (2) When the energy difference between the π^* levels is large (i.e., >0.2 V), then the localized excitation model works well and the emission emanates from a virtually pure state involving the ligand with the lowest π^* energy. (3) As the π^* levels of the various ligands approach each other, mixing occurs and a MOP model is more appropriate. Thus for our systems, if the lowest π^* energy level of the accessory ligand is similar to or below that of the sensing ligand, the accessory ligand will not be "innocent" and may have a significant impact on the observed environmental sensitivity of the complex.

Table 3 shows the quantum yields, radiative and nonradiative rate constants for our suite of complexes as well as comparison values for the appropriate tris complexes. One chooses accessory ligands to enhance some aspect of the reporter complex, and using $[Ru(5\text{-}Et_2Nphen)(phen)_2](ClO_4)_2$ as a reference, we find that ring substitution by CH_3, φ, and Cl all enhance the quantum yield, largely through an increase in k_r. These parameters give no clue that φ and Cl substitution will essentially render the complex pH insensitive. However, the first reduction potentials, a proxy for the π^* energy levels of

dx.doi.org/10.1021/ic201114u | Inorg. Chem. 2012, 51, 3355–3365

Table 3. Quantum Yields, Decay Rate Constants, and Reduction Potentials for $RuL'L_2^{2+}$ and RuL_3^{2+} Complexes[a]

$RuL'L_2^{2+}$	φ[b] $RuL'L_2$	k_r[b] s^{-1}	k_{nr}[b] s^{-1}	φ RuL_3	k_r s^{-1}	k_{nr} s^{-1}	1st red. (V)[c]
$(bpy)_2$	0.048	5.8×10^4	11.5×10^5	0.089[d]	7.7×10^4	7.9×10^5	−1.35[e]
$(Me_2bpy)_2$	0.050	4.7×10^4	9.0×10^5	0.073[f]	9.0×10^4	9.62×10^5	−1.43[f]
$(phen)_2$	0.024	1.7×10^4	6.7×10^5	0.019[d]	4.2×10^4	21.8×10^5	−1.35[e]
$(5\text{-}Et_2Nphen)_2$	0.044	5.0×10^4	10.8×10^5				−1.43
$(Me_4phen)_2$	0.087	5.5×10^4	6.3×10^5	0.032[d]	6.7×10^4	20.2×10^5	<−1.52[e]
$(Me_2phen)_2$	0.070	5.6×10^4	7.4×10^5	0.061[d]	7.2×10^4	11.0×10^5	−1.52[e]
$(5\text{-}Et_2Nphen)(CN)_2$	0.042	2.6×10^4	6.0×10^5				
$(4,7\text{-}Cl_2phen)_2$	0.049	2.4×10^4	4.7×10^5	0.052	3.0×10^4	5.48×10^5	−1.15
$(\varphi_2\text{-}phen)_2$	0.24	5.0×10^4	1.6×10^5	0.37[d]	5.7×10^4	0.99×10^5	−1.22[g]
$(5\text{-}Clphen)_2$	0.053	4.7×10^4	8.4×10^5	0.035[d]	5.2×10^4	14.4×10^5	−1.22[e]
$(\varphi_2\text{-}bpy)_2$	0.16	10.3×10^4	5.5×10^5	0.20[f]	1.3×10^5	5.0×10^5	−1.25[f]

[a] L′ = 5-Et_2Nphen, L = accessory ligand. [b] Values obtained in CH_3OH at 25 °C. [c] Values obtained in CH_3CN at 25 °C. [d] These values taken from ref 3b in EtOH/CH_3OH (4:1) at 20 °C. They represent upper limits as φ for $Ru(bpy)_3Cl_2$ is reported as 0.045 for CH_3OH and 0.069 for EtOH. [e] Ref 3b. [f] Ref 25b. [g] Ref 31.

the ligands, do help provide an explanation for our results. Thus, when the first reduction potential of the accessory ligand is more negative than that of the sensing ligand, the complex is pH sensitive, excitation is more localized on the sensing ligand, and the dynamic range is enhanced . Even when the potentials are similar, (i.e., $\Delta E < 0.1$ V), sufficient mixing or thermal equilibration occurs such that the π^* orbital of the sensing ligand is well represented in the emitting state wave function, conferring pH sensitivity. However, for the Cl and φ substituted accessory ligands, the π^* orbitals are significantly below that of the sensing ligand, and the excitation is largely localized on a pH insensitive accessory ligand.

CONCLUSIONS

Most environmentally sensitive luminescent complexes rely on a modified ligand to perform the analyte recognition and register this event by changes in the luminescence. Many of these complexes also contain additional accessory ligands which can be used to enhance various aspects of the luminescence (i.e., improved quantum yield, color shifts, or lifetime enhancement). The ability to tune the response of Ru(II), Os(II), and Ir(III) complexes through judicious choice of accessory ligands is one the main reason for selecting this type of complex for sensor applications. This work again confirms that significant changes in both dynamic range and pK_a^* can be obtained by judicious choice of accessory ligand. Use of accessory ligands to enhance environmental response is a widely applicable strategy regardless of the target analyte. However, there is a caveat. If the first reduction potential of the accessory ligand, a proxy for the energy of the π^* level, is well below that of the sensing ligand, the response of the complex to the environmental change or analyte may be significantly muted. The simple localized excitation model is a good starting point and largely true for ligands of rather different π^* energies. However, as the π^* levels approach each other, mixing clearly occurs and a more complex model is required. Theory suggests, and our observations support, that ultimately it is the energy difference between the π^* levels of the protonated and non-protonated ligands in comparison with the π^* level of the accessory ligand, coupled with the energy gap law that determines whether the system is or is not environmentally (i.e., pH) responsive.

ASSOCIATED CONTENT

Supporting Information

Further details are given in Figures S1−S4 and Tables S1−S3. This material is available free of charge via the Internet at http://pubs.acs.org.

AUTHOR INFORMATION

Corresponding Author

*E-mail: degrafba@jmu.edu.

Notes

The authors declare no competing financial interest.

ACKNOWLEDGMENTS

It is a pleasure to acknowledge the assistance of the North Carolina State University Chemistry Department's Mass Spectroscopy Facility in obtaining the ES/MS data for our complexes. E.D., M.S., J.B., A.M.W., and B.A.D. wish to acknowledge the Dreyfus Foundation through its Senior Scientist Mentoring Grants Program for valuable support of this research. J.N.D. and B.A.D. wish to acknowledge the National Science Foundation (Grant CHE-04-10061) for partial support of this work. C.T. is grateful to the Body Foundation for computer equipment.

REFERENCES

(1) Extensive reviews include: (a) Wolfbeis, O. S. *Anal. Chem.* **2008**, *80* (12), 4269−4283. (b) Lowery, M.; Fakayode, S. O.; Geng, M. L.; Baker, G. A.; Wang, L.; McCarrol, M. E.; Patonay, G.; Warner, I. M. *Anal. Chem.* **2008**, *80* (12), 4551−4574. (c) De Silva, A. P.; Gunaratne, H. Q. N.; Gunnlaugsson, T.; Huxley, A. J. M.; McCoy, C. P.; Rademacher, J. T.; Rice, T. E. *Chem. Rev.* **1997**, *97*, 1515−1566.

(2) DeGraff, B. A.; Demas, J. N. *Coord. Chem. Rev.* **2001**, *211* (1), 317−335.

(3) (a) Kalyanasundaram, K. *Photochemistry of Polypyridine and Porphyrin Complexes*; Academic Press: San Diego, CA, 1992. (b) Juris, A.; Balzani, V.; Barigelletti, F.; Campagna, S.; Belser, P.; Von Zelewsky, A. *Coord. Chem. Rev.* **1988**, *84*, 85−277.

(4) (a) Lowe, M. P.; Mathieu, C. E.; Parker, D.; Senanayake, P. K.; Kataky, R. *Inorg. Chem.* **2001**, *40*, 5860−5867. (b) Ellerbrock, J. C.; McLoughlin, S. M.; Baba, A. I. *Inorg. Chem. Commun.* **2002**, *5*, 555−559. (c) Gunnlaugsson, T.; Leonard, J. P.; Senechal, K.; Harte, A. J. *J. Am. Chem. Soc.* **2003**, *125*, 12062−12063. (d) Vicente, M.; Bastida, R.; Lodeiro, C.; Macias, A.; Parola, A. J.; Valencia, L.; Spey, S. E. *Inorg. Chem.* **2003**, *42*, 6768−6779. (e) Wong, K. M-C.; Tang, W.-S.; Lu, X.-X.; Zhu, N.; Yam, V. W-W. *Inorg. Chem.* **2005**, *44*, 1492−1498. (f) Ressalan, S.; Iyer, C. S. P. *J. Lumin.* **2005**, *111*, 121−129.

(g) Tzeng, B.-C.; Chen, B.-S.; Chen, C.-K.; Chang, Y.-P.; Tzeng, W.-C.; Lin, T.-Y.; Lee, G.-H.; Chou, P.-T.; Fus, Y.-J.; Chang, A. H-H. *Inorg. Chem.* **2011**, *50*, 5379−5388.
(5) Higgins, B.; DeGraff, B. A.; Demas, J. N. *Inorg. Chem.* **2005**, *44* (19), 6662−6669.
(6) In contrast, the impact of accessory ligands on the emission of cyclometalated Ir(III) complexes has received considerable study. See for example: Li, J.; Djurovich, P. I.; Alleyne, B. D.; Yousfuddin, M.; Ho, N. N.; Thomas, J. C.; Peters, J. C.; Bau, R.; Thompson, M. E. *Inorg. Chem.* **2005**, *44*, 1713−1727 , and references therein.
(7) Caspar, J. V.; Meyer, T. J. *J. Am. Chem. Soc.* **1983**, *105*, 5583−5590.
(8) Sacksteder, L.; Demas, J. N.; DeGraff, B. A. *Inorg. Chem.* **1989**, *28*, 1787−92.
(9) (a) Sullivan, B. P.; Salmon, D. J.; Meyer, T. J. *Inorg. Chem.* **1978**, *17*, 3334−3341. (b) Giordano, P. J.; Bock, C. R.; Wrighton, M. S. *J. Am. Chem. Soc.* **1978**, *100*, 6960−6965. (c) Baggot, J. E.; Gregory, G. K.; Pilling, M. J.; Anderson, S.; Seddon, K. R.; Turp, J. E. *J. Chem. Soc., Faraday Trans. 2* **1983**, *79*, 195−210. (d) Evans, I. P.; Spencer, A.; Wilkinson, G. *J. Chem. Soc., Dalton Trans.* **1973**, 204−209. (e) Zakeeruddin, S. M.; Nazeeruddin, Md. K.; Humphry-Baker, R.; Gratzel, M.; Shklover, V. *Inorg. Chem.* **1998**, *37*, 5251−5259.
(10) (a) Kishnan, S.; Kuhn, D. J.; Hamilton, G. A. *J. Am. Chem. Soc.* **1977**, *99*, 8121−8125. (b) Shen, Y.; Sullivan, B. P. *Inorg. Chem.* **1995**, *34*, 6235−6236. (c) Riklin, M.; Tran, D.; Bu, X.; Laverman, L. E.; Ford, P. C. *J. Chem. Soc., Dalton Trans.* **2001**, 1813−1819.
(11) Snyder, H. R.; Freier, H. E. *J. Am. Chem. Soc.* **1946**, *68*, 1320−1322.
(12) Freedman, D. A.; Evju, J. K.; Pomije, M. K.; Mann, K. R. *Inorg. Chem.* **2001**, *40*, 5711−5715.
(13) Kalyanasundram, K. *Photochemistry of Polypyridine and Porphyrin Complexes*; Academic Press: San Diego, CA, 1992; Chapter 6.
(14) (a) Vos, J. G. *Polyhedron* **1992**, *11* (18), 2285−2299. (b) Wang, R.; Vos, J. G.; Schmehl, R. H.; Hage, R. *J. Am. Chem. Soc.* **1992**, *114*, 1964−1970.
(15) Frish, M. J., et al. *Gaussian 09*, Revision A.02; Gaussian, Inc: Wallingford, CT, 2009.
(16) (a) Lee, C.; Yang, W.; Parr, R. G. *Phys. Rev. B* **1988**, *37*, 785−89. (b) Becke, A. D. *J. Chem. Phys.* **1992**, *96*, 2155−2160. (c) Becke, A. D. *J. Chem. Phys.* **1992**, *92*, 9173−9177. (d) Becke, A. D. *J. Chem. Phys.* **1993**, *98*, 1372−1377. (e) Becke, A. D. *J. Chem. Phys.* **1993**, *98*, 5648−5652.
(17) Andrae, D.; Haeusserman, U.; Dolg, M.; Preuss, H. *Theor. Chem. Acc.* **1990**, *77*, 123−141.
(18) Tomasi, J.; Menucci, B.; Cammi, R. *Chem. Rev.* **2005**, *105*, 2999−3093.
(19) Furche, F.; Ahlrichs, R. *J. Chem. Phys.* **2002**, *117*, 7433−7447.
(20) Murov, S. L. *Handbook of Photochemistry*; Marcel Dekker: New York, N.Y., 1973; p 89.
(21) Clarke, Y.; Xu, W.; Demas, J. N.; DeGraff, B. A. *Anal. Chem.* **2000**, *72*, 3469−3475.
(22) (a) Sun, H.; Hoffman, M. Z. *J. Phys. Chem.* **1993**, *97*, 5014−5018. (b) Casalboni, F.; Mulazzani, Q. G.; Clark, C. D.; Hoffman, M. Z.; Orizondo, P. L.; Perkovic, M. W.; Rillema, D. P. *Inorg. Chem.* **1997**, *36*, 2252−2257.
(23) Ireland, J. F.; Wyatt, P. A. H. *Adv. Phys. Org. Chem.* **1976**, *12*, 131−153.
(24) *Handbook of Chemistry and Physics*, 71st ed; Lide, D. R., Ed.; CRC Press: Boca Raton, FL, 1990; pp 8−33.
(25) (a) Damrauer, N. H.; Cerullo, G.; Yeh, A.; Boussie, T. R.; Shank, C. V.; McCusker, J. K. *Science* **1997**, *275*, 54−61. (b) Damrauer, N. H.; Boussie, T. R.; Devenney, M.; McCusker, J. K. *J. Am. Chem. Soc.* **1997**, *119*, 8253−8268. (c) Damrauer, N. H.; McCusker, J. K. *J. Phys. Chem. A* **1999**, *103*, 8440−8446. (d) Curtright, A. E.; McCusker, J. K. *J. Phys. Chem. A* **1999**, *103*, 7032−7041. (e) Monat, J. E.; McCusker, J. K. *J. Am. Chem. Soc.* **2000**, *122*, 4092−4097.
(26) (a) Bradley, P. G.; Kress, N.; Hornberger, B. A.; Dallinger, R. F.; Woodruff, W. H. *J. Am. Chem. Soc.* **1981**, *103*, 7441−7446. (b) Kober, E. M.; Sullivan, B. P.; Meyer, T. J. *Inorg. Chem.* **1984**, *23*, 2098−2104. (c) Ferguson, J.; Krausz, E. R.; Maeder, M. *J. Phys. Chem.* **1985**, *89*, 1852−1854. (d) Kitamura, N.; Kim, H.-B.; Kawanishi, Y.; Obata, R.; Tazuke, S. *J. Phys. Chem.* **1986**, *90*, 1488−1491. (e) DeArmond, M. K.; Myrick, M. L. *Acc. Chem. Res.* **1989**, *33*, 364−370. (f) Yabe, T.; Orman, L. K.; Anderson, D. R.; Yu, S.-C.; Xu, X.; Hopkins, J. B. *J. Phys. Chem.* **1990**, *94*, 7128−7132.
(27) (a) Smalley, S. J.; Waterland, M. R.; Telfer, S. G. *Inorg. Chem.* **2009**, *48*, 13−15. (b) Juris, A.; Campagna, S.; Balzani, V.; Germaud, G.; von Zelewsky, A. *Inorg. Chem.* **1988**, *27*, 3652−3655. (c) Juris, A.; Barigelletti, F.; Balzani, V.; Belser, P.; von Zelewsky, A. *Inorg. Chem.* **1985**, *24*, 202−206. (d) Barigelletti, R.; Juris, A.; Balzani, V.; Belser, P.; von Zelewsky, A. *Inorg. Chem.* **1983**, *22*, 3335−3339.
(28) (a) Chen, Y.-J.; Xie, P.; Heeg, M. J.; Endicott, J. F. *Inorg. Chem.* **2006**, *45*, 6282−6297. (b) Kumar, C. V.; Barton, J. K.; Gould, I. R.; Turro, N. J.; Van Houten, J. *Inorg. Chem.* **1988**, *27*, 648−651.
(29) Dreuw, A.; Head-Gordon, M. *J. Am. Chem. Soc.* **2004**, *126*, 4007−4016.
(30) (a) Elliot, C. M.; Hershenhart, E. J. *J. Am. Chem. Soc.* **1982**, *104*, 7519−7526. (b) Rillema, D. P.; Allen, G.; Meyer, T. J.; Conrad, D. *Inorg. Chem.* **1983**, *22*, 1617−1622. (c) Mabrouk, P.; Wrighton, M. S. *Inorg. Chem.* **1986**, *25*, 526−531. (d) Wacholtz, W. F.; Auerbach, R. A.; Schmehl, R. H. *Inorg. Chem.* **1986**, *25*, 227−234.
(31) Skarda, V.; Cook, M. J.; Lewis, A. P.; McAuliffe, G. S. G.; Thompson, A. J.; Robbins, D. J. *J. Chem. Soc., Perkin Trans. II* **1984**, 1309−1311.